Perception of Haidinger Brushes in Macular Disease Depends on Macular Pigment Density and Visual Acuity

Philipp L. Müller,[1,2] Simone Müller,[1] Martin Gliem,[1,2] Kristina Küpper,[1] Frank G. Holz,[1,2] Wolf M. Harmening,[1] and Peter Charbel Issa[1,2]

[1]Department of Ophthalmology, University of Bonn, Bonn, Germany
[2]Center for Rare Diseases, University of Bonn, Bonn, Germany

Correspondence: Peter Charbel Issa, Department of Ophthalmology, University of Bonn, Ernst-Abbe-Str. 2, 53127 Bonn, Germany; peter.issa@ukb.uni-bonn.de.

WMH and PCI contributed equally to the work presented here and should therefore be regarded as equivalent authors.

Submitted: December 22, 2015
Accepted: February 20, 2016

Citation: Müller PL, Müller S, Gliem M, et al. Perception of Haidinger brushes in macular disease depends on macular pigment density and visual acuity. *Invest Ophthalmol Vis Sci*. 2016;57:1448–1456. DOI:10.1167/iovs.15-19004

Purpose. To optimize the perceptibility of Haidinger brushes (HB) and to investigate its association with visual acuity and macular pigment density.

Methods. In this prospective cross-sectional study, each subject underwent best-corrected visual acuity (BCVA) testing, funduscopy, and assessment of macular pigment optical density (MPOD) using the two-wavelength fundus autofluorescence method. Haidinger brush visibility was tested with a rotating linear polarizer and a controllable three-color light-emitting diode (LED) panel as light source. A simple model of macular pigment absorption was used to predict HB visibility as a function of stimulus wavelength and MPOD.

Results. All control eyes ($n = 92$) and 34% of the 198 eyes of subjects with macular disease (age-related macular degeneration, $n = 40$; macular telangiectasia type 2, $n = 52$; Stargardt disease, $n = 58$; other retinal dystrophies, $n = 48$) perceived HB when an optimized test setup (464-nm LED light) was applied. The degree of psychophysical perception and the dependency on different wavelengths were in accordance with the absorptance model. In eyes of subjects with macular disease, minimum thresholds of MPOD and BCVA required for HB perception were identified. Subjects with macular telangiectasia type 2 showed lowest values of MPOD and were mostly unable to perceive HB despite relatively preserved BCVA.

Conclusions. Macular pigment and a relatively preserved foveal function are necessary for the perception of HB. Haidinger brushes are usually not perceived by subjects with macular telangiectasia type 2, likely due to their characteristic foveal depletion of macular pigment.

Keywords: Haidinger brush, macular pigment, macular disease, entoptic phenomenon, visual acuity

Haidinger brushes (HB) are named after Wilhelm Karl Ritter von Haidinger, who first described the entoptic phenomenon in several publications between 1844 and 1854.[1–6] Haidinger brushes can be observed when the gaze is directed at the sky or other sources comprising short-wavelength linearly polarized light. When the light source is broadband, the perceptual quality is usually described as a dark-yellowish hourglass-shaped figure flanked by bright bluish spots forming brushes of approximately 4° of visual angle around the locus of fixation.[7–12] If the plane of polarization relative to the eye does not change, the visual phenomenon vanishes after 2 to 3 seconds.[7–10,13,14]

The exact physiological origin of this entoptic phenomenon is not entirely understood, and a few possible explanations have been put forward. What is commonly accepted is that HB visibility requires birefringent structures in the eye. Such double-refracting properties have been described for the xanthophylls lutein, zeaxanthin, and meso-zeaxanthin, which together constitute the macular pigment.[15–21] The location and the size of the HB as well as the illumination wavelength range resulting in maximum psychophysical detection (460–490 nm) correspond well to the distribution and the absorption maximum of the macular pigment.[7–14] However, some authors proposed that the polarization properties of Henle fiber layer around the fovea may also evoke HB visibility.[6,22–25] Furthermore, birefringence of the cornea and distribution and wave-guiding properties in S-cones represent alternative potential explanations.[11,26–30]

Haidinger brushes have been used for diagnosis and pleoptic therapy in amblyopia.[31–36] Also, their perception has been suggested to be a favorable prognostic marker in patients undergoing cataract surgery,[6,7,9,10,31,37–40] as media opacity has limited influence on HB visibility.[41,42] However, studies on the relationship between physiological parameters with the perception of the entoptic phenomenon have been challenging due to a highly variable HB visibility even in healthy subjects.[27,43]

This study describes test conditions that consistently enable healthy subjects to perceive the entoptic phenomenon. Investigations in subjects with various retinal diseases using the same setup then allowed study of the associations of HB visibility with visual acuity and macular pigment optic density.

Methods

This monocenter cross-sectional prospective study was performed between January 2014 and April 2015 at the Department of Ophthalmology of the University of Bonn, Germany. The study was in adherence with the Declaration of

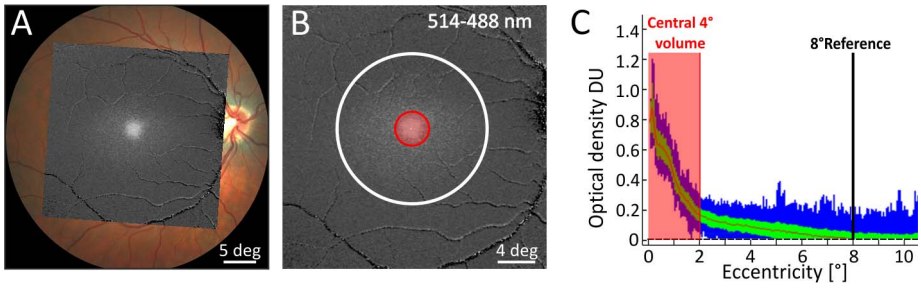

Figure 1. Measurement of macular pigment optic density (MPOD). Fundus photograph (**A**), map of relative MPOD (**A**, **B**), and MPOD as a function of eccentricity (**C**; in density units, DU) are shown for a control eye. (**A**) The relative MPOD map from (**B**) is superimposed onto a normal color fundus photo. (**B**, **C**) The map of relative MPOD is calculated by the formula of Delori[47] using the two-wavelength autoflourescence method with excitation at 488 and 514 nm using a modified Heidelberg Retina Angiograph (HRA classic, Heidelberg Engineering).[47] As Haidinger brushes are described as located approximately 4° of visual angle around the locus of fixation,[7–12] $MPOD_4$ was calculated as sum of all optical densities in the area marked by the *red circle* at 2° eccentricity from the fovea (4° diameter, *shaded in red*) relative to the reference (ring at 8° eccentricity from the fovea, *white*). This is also the volume above the *horizontal dotted line* that is created when the diagram is rotated by the *y*-axis.

Helsinki. Local Institutional Review Board approval was granted (Ethikkommission, Medizinische Fakultät, Rheinische Friedrich-Wilhelms-Universität Bonn), and subjects' informed consent was obtained after explanation of the nature of the study.

Subject Characteristics

Ninety-two eyes of 46 healthy subjects (age, mean 44 years; range, 18–84 years) with no known ocular disease and normal findings on funduscopy, confocal scanning laser ophthalmoscopy (cSLO), and optical coherence tomography (OCT) imaging served as controls. One hundred ninety-eight eyes of 99 subjects with retinal diseases primarily affecting the macula (macular disease, MD; age, mean 54 years; range, 18–86 years) were examined. Among those were subjects diagnosed with macular telangiectasia type 2 (MacTel type 2, $n = 26$), age-related macular degeneration (AMD, $n = 20$), or hereditary retinal dystrophies (Stargardt disease, $n = 29$; other macular or cone/cone–rod dystrophies, $n = 24$). Diagnosis was based on funduscopy, cSLO and OCT imaging, electroretinography (ERG), and, in some instances, molecular genetic testing. Subjects with ocular comorbidities substantially affecting visual function (e.g., significant media opacity, amblyopia, or optic nerve disease) were excluded. Best-corrected visual acuity (BCVA) was tested using ETDRS charts.[44] For analysis and reporting, BCVA was converted to logMAR and had to be $\leq$1.7 logMAR (Snellen equivalent: 20/1000). In addition, patients with MacTel type 2 underwent fundus-controlled microperimetry testing (MP-1; Nidek, Padua, Italy) using a macular grid with 1° distance between testing points.[45,46] Before microperimetry testing and retinal imaging, pupils were dilated by instillation of 0.5% tropicamide and 2.5% phenylephrine. Subjects' characteristics and demographic data are shown in Supplementary Tables S1 and S2.

Measurement of Macular Pigment Optical Density

Macular pigment optical density (MPOD) was determined with the two-wavelength fundus autofluorescence (AF) method described by Delori[47] using a modified Heidelberg Retina Angiograph (HRA classic; Heidelberg Engineering, Heidelberg, Germany). The instrument records two averaged fundus AF images, one with an excitation wavelength at 488 nm and the other at 514 nm, in conjunction with a barrier filter that blocks all wavelengths shorter than 560 nm. Macular pigment absorbs light in the short-wavelength range with a maximum at 460 nm. Therefore, increasing MPOD results in decreasing foveal AF on 488-nm images, but less on 514-nm images since the excitation light at 488 nm is absorbed considerably more than at 514 nm. Subtraction of the two averaged images results in an image representing MPOD distribution.[47] The two-wavelength fundus AF method was shown to be highly reproducible for measuring MPOD.[48,49]

Macular pigment optical density on two-wavelength AF images is commonly measured using the mean gray level along a concentric ring at 6° or 7° eccentricity as a reference, where macular pigment density is very low. However, because patients with MacTel type 2 usually show a depletion of central macular pigment while MPOD may be highest at approximately 6° eccentricity,[50,51] a more eccentric reference ring at 8° was used (Fig. 1).[52] The fovea is defined by the software as the center of the normal Gaussian MPOD distribution. Whenever this definition was not possible, for example, due to very low foveal MPOD, the fovea was localized manually using OCT images as guidance. As a quantitative parameter, mean MPOD in a 4° diameter central area ($MPOD_4$) was analyzed (Fig. 1). Due to the relative calculation of $MPOD_4$ compared to a mean reference gray level at 8° eccentricity, a few cases with computationally negative values of $MPOD_4$ were found (i.e., when the foveal gray level is lower than the reference gray level). The $MPOD_4$ was set to zero in those cases, as it cannot be negative. This was the case in 21 out of 52 eyes with MacTel type 2, in 10 out of 146 eyes with other MDs, and in none of the controls. The $MPOD_4$ is expressed in optical density units (DU).

Haidinger Brush Visibility Testing

As HB visibility vanishes after 2 to 3 seconds if the plane of polarization relative to the eye does not change,[7–10,13,14] we used a polarization filter (Macula Integrity Tester 2; Bernell, Mishawaka, IN, USA) rotating at 2 Hz. It was placed 20 cm away from the eye between the subject and the light source (100-cm total viewing distance, see Fig. 2A). A multicolor 30 × 30 cm light-emitting diode (LED) panel (LED Panel Light, 3030-RGB, LED-SMD-Shop, Coswig, Germany) served as light source. It contains three different types of colored LEDs with emission spectra of ~20- to 30-nm full width at half maximum: blue (464-nm peak wavelength); green (516-nm peak wavelength); and red (632-nm peak wavelength). By controlling the output power of each LED type and selectively combining all three types, 15 different colors were produced. The exact wavelength spectra and radiometric/photometric measurements of each color can be found in Supplementary Figure S1. Haidinger brush visibility was tested at each color in a two-alternative forced-choice experiment, in which subjects were asked to

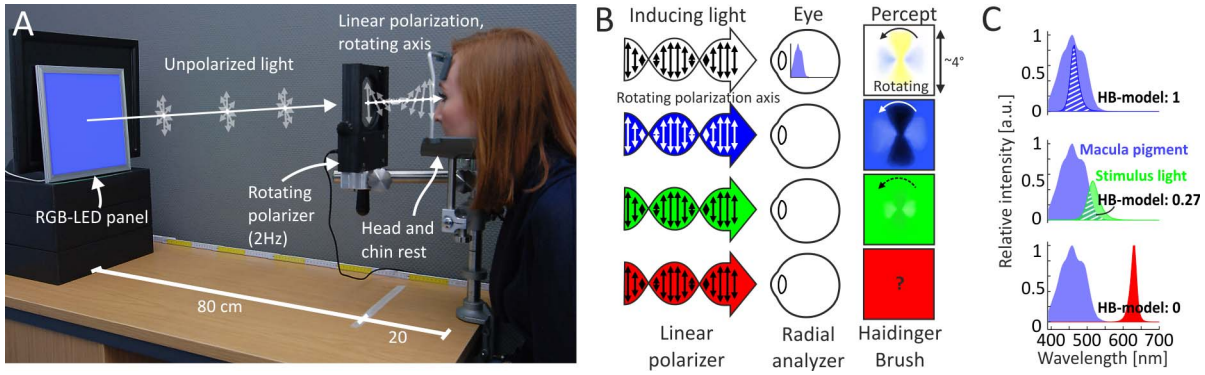

Figure 2. Experimental setup for Haidinger brush visibility testing and macular pigment absorptance model. (**A**) Subjects viewed a colored panel through a filter that transmits light at only a single polarization axis. When the filter is rotated (at 2 Hz in our experiments), the percept of a rotating Haidinger brush emerges, with its visibility dependent on the colors used as light source. (**B**) The hypothesis put forward here is that Haidinger brush visibility is modulated by the amount of macula pigment present in the retina (absorption spectrum between 400 and 550 nm), acting as a weighted radial analyzer. (**C**) A model of Haidinger brush visibility (HB-model) was derived by calculating the relative absorption of the stimulus light by macula pigment as a fraction of the total light incident on the retina. In the given example, blue receives the highest value, because the entire stimulus light is screened by macula pigment. Red has an HB-model value equaling zero because all stimulus light lies outside the screenable spectrum.

report the direction of rotation of the HB (Supplementary Tables S1 and S2).

Macular Pigment Absorption Model

In order to better understand the relationship between the possible role of macular pigment for the visibility of HB in healthy controls, and to project HB visibility to cases of MD, a simple model of relative light absorptance was utilized. The model assumes that HB visibility manifests by a selective filtering of polarized light as a function of the angle between the linear polarization axis and the birefringent retinal structures. First, known combined absorption spectra of retinal macular pigments were digitized and normalized from Figure 1 of Sharpe and colleagues.[53] The product of normalized pigment absorptance and wavelength spectrum of the colors used in the HB visibility setup (Supplementary Fig. S1) was calculated, and the area under that curve was used to arrive at a quantitative description of a maximally HB visibility–inducing effect (HB-model-I). Some predictions about wavelength dependence and the influence of pigment density can be made with such an approach. With blue light, for instance, relative pigment absorption would be maximal, and a darker brush-like area within a blue background would be visible with a healthy retina (compare Fig. 2B). Haidinger brush visibility in this condition will be linearly scaled down in cases where pigment density is decreased, because less light is screened. When longer visible wavelengths are present that are unfiltered by macular pigment, HB visibility will be masked. Wavelengths that do not fully overlap with the macular pigment absorption spectrum (e.g., green light) will have both an inducing and a masking effect, dependent on how much energy falls into either category. Red light, on the other end of the spectrum, does not interact with macular pigment and thus HB should not be visible. To account for such a wavelength-dependent HB visibility masking effect, a final model value of HB visibility (HB-model) was calculated as the fraction of HB-model-I and the total irradiance of the background light (Fig. 3C). For color 7 (magenta), for example, the amount of light screened by pigment is approximately half of the total irradiance incident on the retina (Supplementary Fig. S1), and the model produces, correspondingly, a value of 0.45. To estimate the general visibility of HB in a tested eye across colors, an HB visibility score was assigned to each color tested. The score is calculated by (1 + 1 − HB model). For a given eye, the HB visibility index was calculated by summing up all individual scores across colors where HB was seen. Hence, an index of 0 denotes that HB was never seen, and a score of 1 indicates that HB was seen with blue light only. Higher indices indicate perception of HB at more challenging background lights (compare Figs. 3B, 7A). Thus, if all colors had been seen, the score would have been 23.8.

It is important to note that a complete description of the perceptual consequences of different wavelength compositions that are dynamically filtered by a rotating linear polarizer might involve a more detailed consideration of both physical and psychophysical principles of color vision (e.g., cone color contrast, time scale of cone adaptation), and is beyond the scope of the current study. Nevertheless, our simplified model produces values that are in agreement with psychophysical results in normal and diseased eyes (see Results).

Data Analysis

To assess a possible association between $MPOD_4$, BCVA, and the HB visibility at different colors, the parameters were compared within and between controls and subjects with MDs. Statistical analysis was performed with commercially available statistical software (Prism 6.0; GraphPad Software, Inc., La Jolla, CA, USA) using one-factor analysis of variance (ANOVA) followed by Tukey's test for the pairwise comparison of groups. Confidence intervals (95%) for subjects' HB visibility were calculated by using the Wilson score interval. The impact of influential factors was evaluated by multivariable linear regression models with R (R Foundation for Statistical Computing, Vienna, Austria).

Results

Using blue LED light in our experimental setup (color # 15; 464 nm; 126 cd/m^2), all healthy control subjects were able to perceive the entoptic phenomenon with both eyes ($n = 94$). None of the subjects described the visual phenomenon when red light was used (color #1; 632 nm; 368 cd/m^2). The other 13 colors employed (see Supplementary Fig. S1 for spectral composition and stimulus luminance) resulted in intermediate HB visibility. When the colors were ordered corresponding to HB visibility, a monotonically increasing visibility function

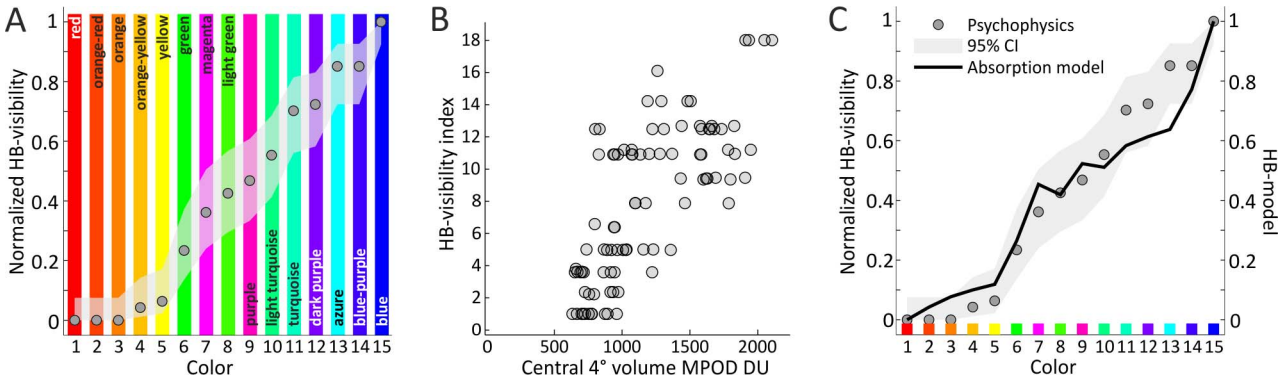

Figure 3. Haidinger brush visibility as a function of stimulus light and macular pigment optical density in healthy subjects. (**A**) Normalized HB visibility in 47 normal subjects for each color used in the experiments, ordered by their visibility value. While none of the subjects could perceive Haidinger brushes at color 1 (red), all subjects could see them at color 15 (blue). The *gray shaded area* is the 95% confidence interval derived from a Wilson score test. Background bar coloring and ordinary color names given here are only for reference. For exact spectral composition of each light, compare Supplementary Figure S1. (**B**) When plotted separately per eye, a clear trend emerges that higher MPOD leads to better HB visibility across test colors. Plotted on the ordinate is an HB visibility index, calculated as the inverse cumulative normalized HB visibility derived from the data set in (**A**), such that eyes perceiving HB with colors farther away from blue receive higher values (Supplementary Table S1). (**C**) Same as in (**A**), now with the prediction of the macular pigment absorptance model (HB-model) shown as *black line* (see Methods and Fig. 2). The mean absolute deviation of model data from behavioral data is 6.5% and lies well within the mean Wilson score interval (13.7% deviation, compare also Fig. 7C).

emerged (Fig. 3A). Moreover, there was a positive correlation between HB visibility and $MPOD_4$ in individuals. Subjects with higher $MPOD_4$ could generally perceive the entoptic phenomenon more easily (Fig. 3B). A model of HB visibility based on the inducing wavelength and macular pigment absorption was constructed (see Methods) and compared to the psychophysical data (Fig. 3C). The model showed a very similar graduated increment in HB-model when the same order of colors was used. The mean absolute deviance from the psychophysical data was 6.5% HB-model, below the mean confidence interval of the psychophysical data, amounting to approximately 13.7% HB visibility deviation. Based on these results we deemed the experimental setup suited to test the impact of MPOD and visual acuity on HB visibility in the diseased retina.

Using the optimized conditions (blue LED light) at which HB visibility was 100% in controls, HB visibility in all investigated subjects with MD was 34% (67/198 eyes). As macular pigment appears to be associated with the perception of the entoptic phenomenon (see above), we investigated if $MPOD_4$ levels were associated with HB visibility in these subjects. The $MPOD_4$ levels were not different between controls and patients perceiving HB (mean deviation [md] [95% confidence interval (CI)]: −18.64 [−140.5, 103.2], $P = 0.9309$). However, these two groups revealed significantly different $MPOD_4$ levels compared to patients not perceiving the entoptic phenomenon (md [95% CI]; controls: 957.6 [854.6, 1061], $P < 0.0001$; patients with HB perception: 976.2 [861.8, 1091], $P < 0.0001$; Fig. 4). Moreover, Figure 4 suggests that there is a lower limit of $MPOD_4$ in patients and controls below which HB cannot be perceived (dashed line at 600 DU).

Next, we investigated the dependency of HB perception from BCVA in MD. When individual $MPOD_4$ levels of all patients' eyes are plotted against BCVA, eyes with HB perception (blue; Fig. 5A) can be well differentiated from eyes with no HB perception (red; Fig. 5A). The minimum $MPOD_4$ threshold necessary for HB visibility is illustrated by the horizontal dashed line ($MPOD_4$ approximately 600 DU), independent from BCVA. In addition, the graph reveals that visibility of HB requires a minimum foveal function (vertical dotted line at BCVA 0.6 logMAR). Eyes with apparently sufficient $MPOD_4$ but no HB perception always had a BCVA > 0.6 logMAR (red circles).

In multivariate analysis (taking HB perception as a dependent variable and age, BCVA, and $MPOD_4$ as independent variables), a statistically significant influence of BCVA ($P < 0.0001$) and $MPOD_4$ ($P < 0.0001$) on HB perception was also identified. However, age did not show any statistically significant impact ($P = 0.627$).

Figures 5B through 5D show the same data as in Figure 5A arranged according to different disease entities. Patients with

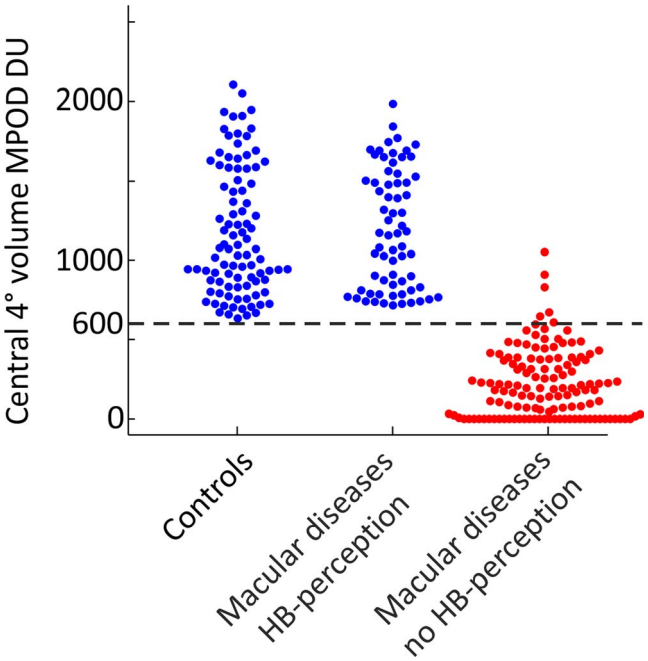

Figure 4. Haidinger brush perception and macular pigment optical density (MPOD) in macular disease. Scatterplot shows central 4° volume MPOD of controls (*black*) and patients with macular disease (MD, contingent with HB perception at color # 15 (*blue*). Markers are individual eyes. Eyes that revealed no HB perception showed reduced MPOD compared to eyes with HB perception and controls, suggesting a dependency of HB visibility on MPOD. *Dashed line* revealed the lower limit of MPOD (600 DU) below which the entoptic phenomenon was not perceived. Negative MPOD values were set to zero.

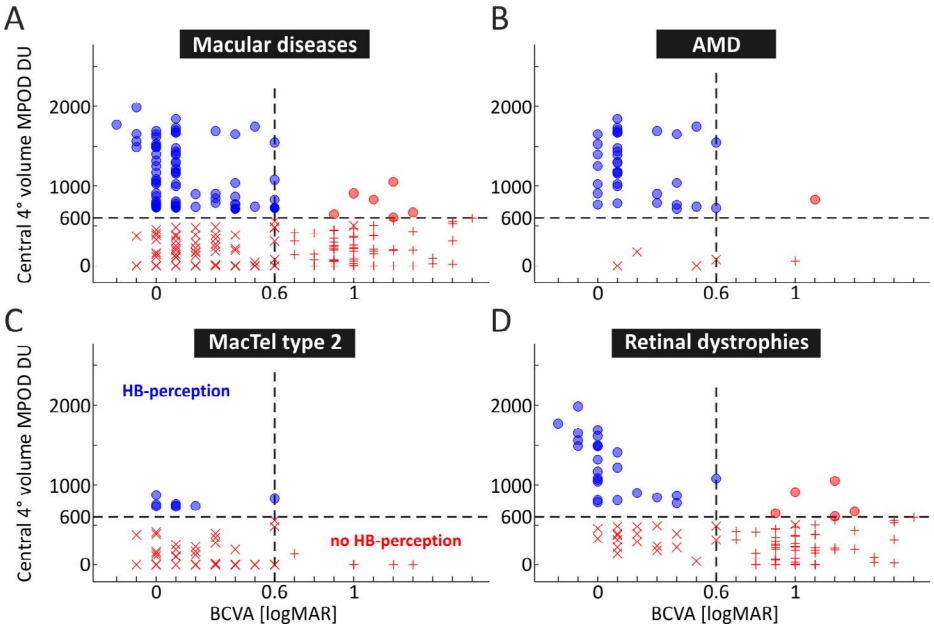

Figure 5. Dependency of Haidinger brush visibility on best-corrected visual acuity (BCVA) and macular pigment optical density (MPOD). Eyes of patients with macular disease that had HB perception (*blue*) or no HB perception (*red*) are plotted according to the BCVA (logMAR, *x*-axis) and central 4° volume MPOD (*y*-axis). (**A**) shows all eyes with macular disease, whereas (**B**–**D**) demonstrates findings in individual entities. Eyes with and without HB perception can be distinctly separated by dividing the plot into four quadrants: On the *y*-axis, a minimum threshold at 600 DU central 4° volume MPOD could be found, enabling HB perception. On the *x*-axis, a minimum visual acuity of 0.6 (logMAR) was found to enable HB perception. This suggests a direct dependency of BCVA and MPOD on HB visibility. Usually, no HB perception occurs in the case low MPOD and impaired BCVA (*red crosses* and *X*s). Only few cases were found with preserved MPOD but reduced BCVA (*red circles*). No HB perception despite relatively preserved BCVA but particularly low MPOD levels (*red X*s) was mostly due to perifoveal atrophy with foveal sparing in patients with age-related macular degeneration (AMD) and retinal dystrophies (**B**, **D**). In addition, a high portion of patients with macular telangiectasia type 2 (MacTel type 2; **C**) can be found within this quadrant, implicating early loss of MPOD before significant loss of BCVA. Hence, only patients with wedge-shaped loss of MPOD but preserved central MPOD could perceive the entoptic phenomenon. Negative MPOD values were set to zero.

AMD (Fig. 5B) mostly perceived the entoptic phenomenon (34 of 40 eyes [85%], all early and intermediate AMD). No HB perception occurred in eyes with relatively preserved BCVA but particularly low $MPOD_4$ levels (4 of 40 eyes, 10%) and in eyes with low BCVA due to late AMD stages (2 of 40 eyes, 5%). Patients with MacTel type 2 (Fig. 5C) were usually not able to perceive the entoptic phenomenon (44 of 52 eyes; 85%) even though most eyes had a BCVA $\leq$ 0.6 logMAR (48 of 52 eyes, 92%). MacTel type 2 patients revealed significantly lower $MPOD_4$ compared to the other MD patients (md [95% CI]: −453.0 [−633.2, −272.8], $P < 0.0001$). Only eyes with loss of macular pigment limited to a wedge-shaped area temporal to

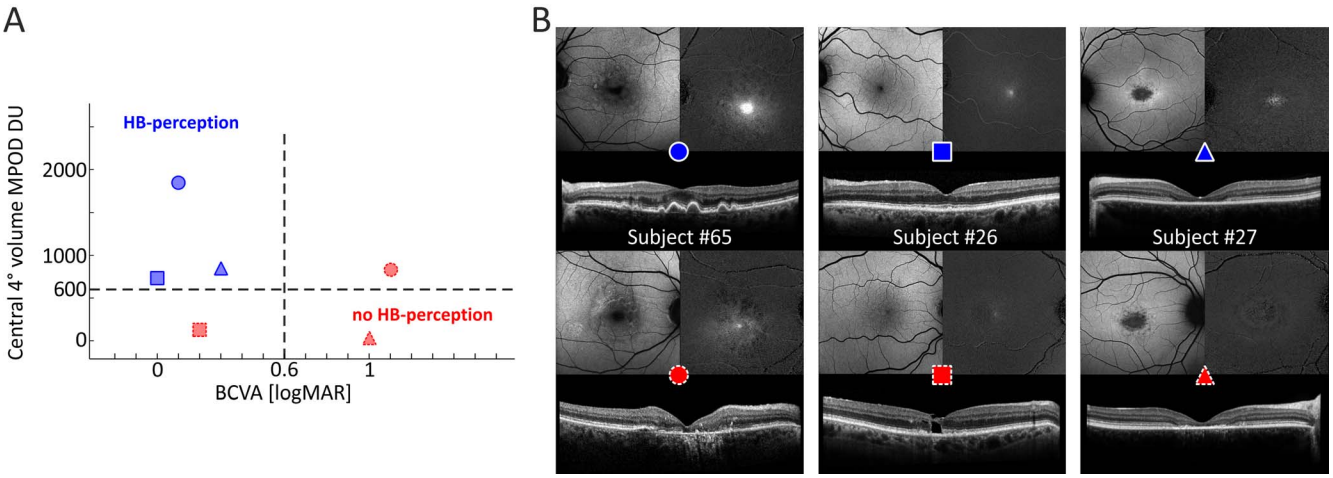

Figure 6. Interocular comparison of three exemplary patients with monocular perception of Haidinger brushes (HB). (**A**) In the scatter plot the eyes of three patients (*symbols*) with monocular HB perception are plotted according to their BCVA and central 4° volume MPOD (as in Fig. 5). (**B**) Fundus autofluorescence images, map of relative MPOD, and horizontal OCT line scan provided for the eye with HB perception (*top row*) and the eye without HB perception (*bottom row*) of the respective three patients (*column*). Nonperception of HB occurred because of structural alteration leading to loss of BCVA (patient #65 with age-related macular degeneration, *circle*), reduced MPOD (patient #26 with macular telangiectasia type 2, *square*), or both low BCVA and low MPOD (patient #27 with a macular dystrophy, *triangle*).

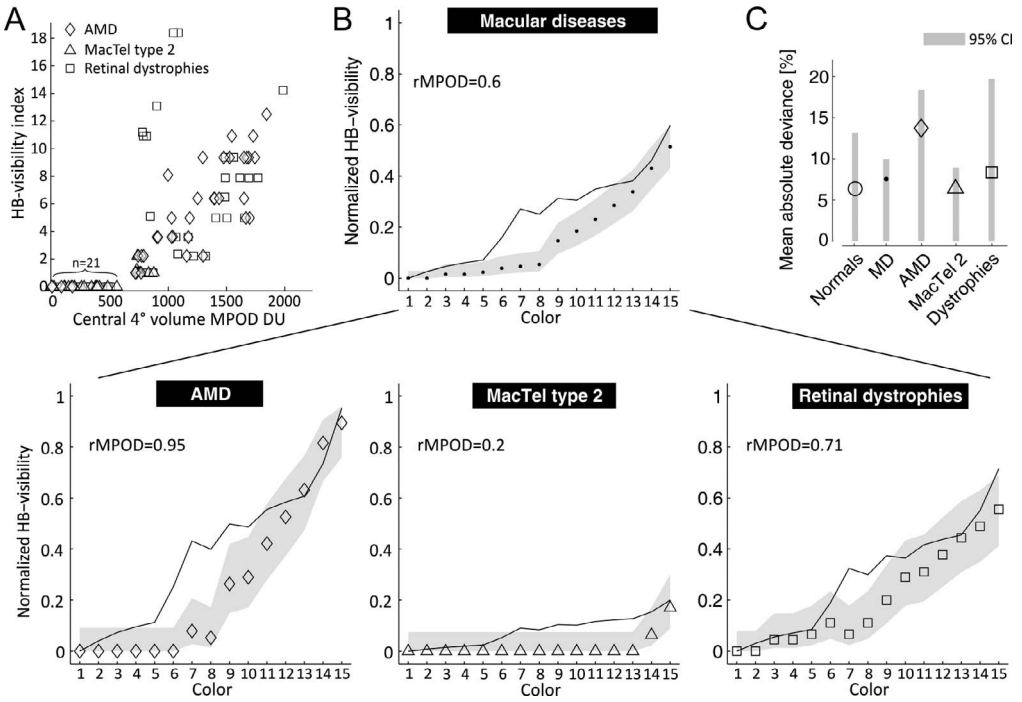

Figure 7. HB visibility for stimulus colors follows absorptance model of MPOD. (**A**) A similar trend as in control subjects emerges that more MPOD leads to better HB visibility across test colors. Plot conventions are as in Figure 3B (Supplementary Table S2). (**B**) Symbols represent experimental data of HB visibility found in our setup. The *gray area* is the 95% confidence interval (Wilson score interval). *Lines* are predictions from the macular pigment absorptance model (see Methods and Fig. 3C). Within the confidence limits governed by number of subjects, the model predicts experimental outcomes well. rMPOD values are the mean MPOD values relative to controls in each disease group. Subjects with BCVA $\leq$ 0.6 (logMAR) were used for this analysis. (**C**) The mean absolute deviances between HB-model and HB perception (psychophysical) were lower than the 95% Wilson score intervals for the behavioral data in each group. *Symbols* represent data from eyes according to disease groups as in (**A**) and (**B**).

the foveal center but relatively preserved central MPOD and BCVA (see below and Fig. 6) could perceive the entoptic phenomenon. As paracentral scotomata are the characteristic functional deficit in this disease,[46,54] microperimetry data were available for all investigated eyes and revealed that presence or absence of a paracentral scotoma was not associated with HB perception (Supplementary Table S2). In monogenetic macular and cone–rod dystrophies (Fig. 5D), the entoptic phenomenon was not perceived if $MPOD_4$ levels were below 600 DU, irrespective of a BCVA $>$ 0.6 logMAR (56 of 106 eyes, 53%) or $\leq$ 0.6 logMAR (20 of 106 eyes, 19%). The latter was usually associated with retinal atrophy involving the central 4°, but a small foveal sparing. Haidinger brushes were also not perceived by a small subset of eyes with retinal dystrophy that showed relatively preserved $MPOD_4$ within an area of severely altered retinal structure associated with reduced BCVA (5 of 106 eyes, 5%).

Patients with HB perception in one eye but not the other (n = 11, Supplementary Table S2; Fig. 6) consistently perceived the entoptic phenomenon only with the eye that had BCVA and $MPOD_4$ within the above-described limits of 0.6 logMAR and $MPOD_4$ 600 DU, respectively. In the fellow eyes, one of the two parameters or both were below these thresholds. Of note, apart from foveal atrophy and/or low $MPOD_4$ levels, right and left eyes were otherwise similar in those cases.

When $MPOD_4$ was plotted against a quantitative measure of HB visibility across test colors for each diseased eye separately, a trend similar to that in controls was observed (Fig. 7A). Eyes with $MPOD_4$ $<$ 600 DU were not able to see the entoptic phenomenon. Higher levels of $MPOD_4$ were associated with better HB visibility across test colors; that is, difficult test conditions (e.g., at color # 5, yellow) were seen only by eyes with higher $MPOD_4$ levels. When the lower levels of $MPOD_4$ observed in eyes with MD were used in the macular pigment absorption model, a clear correspondence to psychophysical tests of HB visibility within the disease groups was found (Fig. 7B). In subjects diagnosed with MacTel type 2, the lowest levels of HB-model were predicted, in accordance with results from psychophysical testing. Combined and individual comparison of the remaining disease groups showed a similar agreement. The mean absolute deviances of HB-model predicted by the model from psychophysical data were all smaller than the 95% Wilson score intervals in each group (controls: 6.4% vs. 13.2%, MacTel type 2: 6.6% vs. 9.0%, AMD: 13.7% vs. 18.5%, dystrophies: 8.4% vs. 19.8%; compare also Fig. 7C).

Discussion

The physiological origin of HB has remained a matter of debate since the first description of the entoptic phenomenon.[5,17,27,28,55–59] This is in part due to the fact that the phenomenon can be experienced only subjectively and is generally of a subtle nature.[7–12] The test conditions used here—bright blue LED light with a spectrum that completely lies within the absorption spectrum of macular pigment—were in favor of a strong subjective effect and allowed us to develop quantitative means to relate its presence with other physiological parameters.

In investigating subjects affected by defined pathologies of the central retina but without ocular comorbidities potentially affecting visual function, changes of HB visibility could be directly related to alterations of the central retina. Specifically, our results allow the following five main conclusions:

1. A minimum macular pigment density appears to be required for the perception of HB. This was observed independent from the underlying disease. In addition, our psychophysical results of HB visibility using a set of different background colors and the accordance with a simple model of macular pigment absorptance support the hypothesis that macular pigment may indeed be the major component underlying the entoptic phenomenon.[7–21] Higher MPOD leads to better HB visibility across test colors in healthy and diseased eyes. To the best of our knowledge, this is the first description of directly associated MPOD measurements with HB perception.
2. A minimum visual acuity of 0.6 logMAR (Snellen equivalent: 20/80) appears necessary to enable visibility of HB. Since we focused on subjects with defined MDs, visual impairment was directly related to foveal alterations. Earlier studies used different experimental setups and often looked at a multitude of ophthalmic alterations. Both may have had an impact on BCVA and HB visibility that makes comparison difficult.[6,7,9,10,37–40] In studies dealing with HB visibility and lens opacity, subjects who were able to perceive HB generally had BCVA $\leq$ 0.6 logMAR after cataract surgery, in accordance with our results.[9,37]
3. Significant differences in BCVA and $MPOD_4$ in patients who were able to perceive HB in only one eye confirmed the importance of foveal integrity and macular pigment for the entoptic phenomenon. Of note, the eye with better visual function and/or more macular pigment of these patients provides an internal control, excluding other interindividual factors that would lead to an inability to perceive HB.[60]
4. Age appears to have a negligible effect on HB perception in our setup. Subjects with AMD as well as the oldest controls were all able to perceive HB as long as macular pigment and visual acuity were within required limits. Concerning HB visibility, previous studies did not focus on age dependency.
5. MacTel type 2 is a disease characterized by a progressive depletion of central macular pigment.[52,54] Almost all patients with this disease were not able to perceive HB, even when visual acuity was normal. Haidinger brush perception was only rarely possible when macular pigment loss was restricted to a paracentral area, with significantly preserved foveal MPOD (in line with a previous case series[60]). Thus, failure to perceive HB in an optimized setup may indicate the disease, especially in patients with low reading ability despite relatively inconspicuous macular changes. In contrast, if a patient perceives HB, the diagnosis of MacTel type 2 is unlikely. We note, though, that objective MPOD measurements may be preferred given the inherent variability in psychophysical testing results.

Limitations of our study mainly involve the assessment of MPOD. Negative foveal MPOD levels—as mainly observed in patients with MacTel type 2—may suggest that the reference was not placed eccentrically enough. In this disease, preserved or possibly even increased MPOD is observed at an eccentricity of approximately 6° to 7°, and an influence on the reference level at 8° may result in underestimation of foveal MPOD. In this study we have not chosen a more eccentric reference because imaging artifacts increase toward the borders of the image. Another factor that may introduce noise in our MPOD measures is increasing lens opacity with age, which may result in decreasing MPOD estimates.[41] We have excluded all subjects with significant cataract to avoid this influence on MPOD measurements. Furthermore, central atrophy of the retinal pigment epithelium may interfere with the two-wavelength AF measurement, leading to misinterpretation of MPOD levels, as the AF signal is very low in these areas independent from the wavelength and the existence of macular pigment. However, low BCVA sufficiently explained failure to perceive the visual phenomenon in these cases.

In this study, precise localization of the preferred retinal locus and an in-depth analysis of foveal pathologic changes (including those in Henle fiber layer) were not performed. Thus, fixation testing and standardized OCT analysis may be included in future studies. We have also not determined other factors that may potentially influence HB perception, such as corneal birefringence.[11,27,28] However, the fact that all controls and all patients with MPOD and BCVA above a certain threshold were able to perceive HB suggests that the effect of such additional factors would at most be minor.

In summary, we have optimized conditions for HB perception testing, such that individuals with healthy eyes are consistently able to perceive the entoptic phenomenon. In patients with MDs, the results indicate that HB perception is dependent on macular pigment density and foveal function.

Acknowledgments

Supported by the ProRetina Deutschland, Aachen, Germany; the German Research Foundation (DFG Ha 5323/5-1; WMH); and the Carl Zeiss Förderfonds (WMH). The Department of Ophthalmology, University of Bonn, receives imaging devices from Heidelberg Engineering, Zeiss, and Optos. The sponsor or funding organization had no role in the design or conduct of this research.

Disclosure: **P.L. Müller**, None; **S. Müller**, None; **M. Gliem**, None; **K. Küpper**, None; **F.G. Holz**, Heidelberg Engineering (C); **W.M. Harmening**, None; **P. Charbel Issa**, None

References

1. Haidinger W. Über das direkte Erkennen des polarisierten Lichts. *Ann der Phys und Chemie*. 1844;63(29).
2. Haidinger W. Über komplimentäre Farbeindrücke bei Beobachtung der Lichtpolarisationsbüschel. *Ann der Phys und Chemie*. 1846;67(435).
3. Haidinger W. Beobachtung der Lichtpolarisationsbüschel in geradlinig polarisiertem Licht. *Ann der Phys und Chemie*. 1846;68(73).
4. Haidinger W. Beobachtung der Lichtpolarisationsbüschel auf Flächen, welche das Licht in zwei senkrecht aufeinander stehenden Richtungen polarisierten. *Ann der Phys und Chemie*. 1846;68(305).
5. Haidinger W. Einige neuere Ansichten über die Natur der Polarisationsbüschel. *Ann der Phys und Chemie*. 1854; 96(314).
6. Goldschmidt M. A new test for function of the macula lutea. *Arch Ophthalmol*. 1950;44:129–135.
7. Forster H. The clinical use of the Haidinger's brushes phenomenon. *Am J Ophthalmol*. 1954;38:661–665.
8. Snodderly DM, Auran JD, Delori FC. The macular pigment. II. Spatial distribution in primate retinas. *Invest Ophthalmol Vis Sci*. 1984;25:674–685.
9. Dodt E, Tsuyama Y, Kuba M. Sensorische und elektrische Antworten bei Reizung der Makula im kurzwelligen (407-527 nm) linear polarisierten Licht (Haidinger-Polarisationsbüschel). *Ophthalmologe*. 1994;91:169–175.
10. Naylor EJ, Stanworth A. The measurement and clinical significance of the Haidinger effect. *Trans Opthal Soc U K*. 1955;75:67–79.

11. Le Floch A, Ropars G, Enoch J, Lakshminarayanan V. The polarization sense in human vision. *Vision Res*. 2010;50:2048–2054.
12. Coren S. The use of Haidinger's brushes in the study of stabilized retinal images. *Behav Res Meth Instru*. 1971;3:295–297.
13. De Vries H, Jielof R, Spoor A. Properties of the human eye with respect to linearly and circularly polarized light. *Nature*. 1950;166:958–959.
14. Manor RS. Entoptic [corrected] phenomena in pregeniculate and postgeniculate hemianopsia with splitting of macula by perimetry. *Am J Ophthalmol*. 1989;108:585–591.
15. Trieschmann M, van Kuijk FJGM, Alexander R, et al. Macular pigment in the human retina: histological evaluation of localization and distribution. *Eye (Lond)*. 2008;22:132–137.
16. Trieschmann M, Beatty S, Nolan JM, et al. Changes in macular pigment optical density and serum concentrations of its constituent carotenoids following supplemental lutein and zeaxanthin: the LUNA study. *Exp Eye Res*. 2007;84:718–728.
17. Bone RA, Landrum JT, Cains A. Optical density spectra of the macular pigment in vivo and in vitro. *Vision Res*. 1992;32:105–110.
18. Bone RA, Landrum JT, Fernandez L, Tarsis SL. Analysis of the macular pigment by HPLC: retinal distribution and age study. *Invest Ophthalmol Vis Sci*. 1988;29:843–849.
19. Sommerburg OG, Siems WG, Hurst JS, Lewis JW, Kliger DS, van Kuijk FJ. Lutein and zeaxanthin are associated with photoreceptors in the human retina. *Curr Eye Res*. 1999;19:491–495.
20. Bernstein PS, Khachik F, Carvalho LS, Muir GJ, Zhao DY, Katz NB. Identification and quantitation of carotenoids and their metabolites in the tissues of the human eye. *Exp Eye Res*. 2001;72:215–223.
21. Whitehead AJ, Mares JA, Danis RP. Macular pigment: a review of current knowledge. *Arch Ophthalmol*. 2006;124:1038–1045.
22. Bone RA, Landrum JT. Macular pigment in Henle fiber membranes: a model for Haidinger's brushes. *Vision Res*. 1984;24:103–108.
23. Hemenger RP. Dichroism of the macular pigment and Haidinger's brushes. *J Opt Soc Am*. 1982;72:734–737.
24. Dimmer F. Ueber die entoptischen Erscheinungen in der Gegend der Macula lutea. *Zentralblatt für Physiol*. 1894;7:266.
25. von Tschermak-Seysenegg A. *Einführung in de Physiologische Optik*. 2nd ed. Vienna: Julius Springer; 1947;142–143.
26. Hecht E. *Optics*. 4th ed. Boston, MA: Addison Wesley; 2002.
27. Temple SE, McGregor JE, Miles C, et al. Perceiving polarization with the naked eye: characterization of human polarization sensitivity. *Proc R Soc B*. doi:10.1098/rspb.2015.0338.
28. Rothmayer M, Dultz W, Frins E, Zhan Q, Tierney D, Schmitzer H. Nonlinearity in the rotational dynamics of Haidinger's brushes. *Appl Opt*. 2007;46:7244–7251.
29. Hochheimer BF, Kues HA. Retinal polarization effects. *Appl Opt*. 1982;21:3811–3818.
30. Hochheimer BF. Polarized light retinal photography of a monkey eye. *Vision Res*. 1978;18:19–23.
31. Cüppers C. Moderne Schielbehandlung. *Klin Monbl Augenheilkd Augenarztl Fortbild*. 1956;129:579–604.
32. Cüppers C. Moderne Schielbehandlung. *Dtsch Med J*. 1958;9:397–401.
33. Cüppers C. Ergebnisse der pleoptischen Therapy unter besonderer Berucksichtigung der Dauerresultate. II. *Doc Ophthalmol*. 1967;23:570–605.
34. Cüppers C. Ergebnisse der pleoptischen Therapy unter besonderer Berucksichtigung der Dauerresultate. *Doc Ophthalmol*. 1967;23:547–549.
35. Adelstein FE, Cüppers C. Le traitement de la correspondance retinienne anormale à paide de prismes. *Ann Ocul (Paris)*. 1970;203:445–457.
36. Thomas C, Spielmann A, Bernardini D. Erfahrungen bei der Amblyopie mit exzentrischer Fixation durch Veränderungen des Innervationsimpulses äußerer Augenmuskeln mittels Prismen und chirurgischen Eingriffen nach den von Cüppers aufgestellten Prinzipien. *Klin Monbl Augenheilkd*. 1975;167:157–162.
37. Sherman M, Priestley B. The Haidinger brush phenomenon: a new clinical use. *Am J Ophthalmol*. 1962;54:807–812.
38. Schmidt I. Diagnostic value of foveal entoptic phenomena in glaucoma. *AMA Arch Ophthalmol*. 1954;52:583–597.
39. Sloan LL, Naquin HA. A quantitative test for determining the visibility of the Haidinger brushes: clinical applications. *Am J Ophthalmol*. 1955;40:393–406.
40. Priestley BS, Foree K. Clinical significance of some entoptic phenomena. *AMA Arch Ophthalmol*. 1955;53:390–397.
41. Sasamoto Y, Gomi F, Sawa M, Sakaguchi H, Tsujikawa M, Nishida K. Effect of cataract in evaluation of macular pigment optical density by autofluorescence spectrometry. *Invest Ophthalmol Vis Sci*. 2011;52:927–932.
42. Sharifzadeh M, Obana A, Gohto Y, Seto T, Gellermann W. Autofluorescence imaging of macular pigment: influence and correction of ocular media opacities. *J Biomed Opt*. 2014;19:96010.
43. Grebe-Ellis J. Zum Haidinger-Büschel. In: Deutsche Physikalische Gesellschaft (DPG). *Didaktik der Physik. Vorträge der Frühjahrstagung der DPG*. Leipzig; 2002:1–11.
44. Early Treatment Diabetic Retinopathy Study design and baseline patient characteristics. ETDRS report number 7. *Ophthalmology*. 1991;98(5 suppl):741–756.
45. Charbel Issa P, Helb H-M, Rohrschneider K, Holz FG, Scholl HPN. Microperimetric assessment of patients with type 2 idiopathic macular telangiectasia. *Invest Ophthalmol Vis Sci*. 2007;48:3788–3795.
46. Heeren TFC, Clemons T, Scholl HPN, Bird AC, Holz FG, Charbel Issa P. Progression of vision loss in macular telangiectasia type 2. *Invest Ophthalmol Vis Sci*. 2015;56:3905–3912.
47. Delori FC. Autofluorescence method to measure macular pigment optical densities fluorometry and autofluorescence imaging. *Arch Biochem Biophys*. 2004;430:156–162.
48. Creuzot-Garcher C, Koehrer P, Picot C, Aho S, Bron AM. Comparison of two methods to measure macular pigment optical density in healthy subjects. *Invest Ophthalmol Vis Sci*. 2014;55:2941–2946.
49. Trieschmann M, Heimes B, Hense HW, Pauleikhoff D. Macular pigment optical density measurement in autofluorescence imaging: comparison of one- and two-wavelength methods. *Graefes Arch Clin Exp Ophthalmol*. 2006;244:1565–1574.
50. Helb H-M, Charbel Issa P, van der Veen RLP, Berendschot TTJM, Scholl HPN, Holz FG. Abnormal macular pigment distribution in type 2 idiopathic macular telangiectasia. *Retina*. 2008;28:808–816.
51. Charbel Issa P, van der Veen RLP, Stijfs A, Holz FG, Scholl HPN, Berendschot TTJM. Quantification of reduced macular pigment optical density in the central retina in macular telangiectasia type 2. *Exp Eye Res*. 2009;89:25–31.
52. Zeimer MB, Spital G, Heimes B, Lommatzsch A, Pauleikhoff D. Macular telangiectasia–changes in macular pigment optical density during a 5-year follow-up. *Retina*. 2014;34:920–928.
53. Sharpe LT, Stockman A, Knau H, Jägle H. Macular pigment densities derived from central and peripheral spectral sensitivity differences. *Vision Res*. 1998;38:3233–3239.
54. Charbel Issa P, Gillies MC, Chew EY, et al. Macular telangiectasia type 2. *Prog Retin Eye Res*. 2013;34:49–77.

Investigative Ophthalmology & Visual Science

55. Bone RA. The role of the macular pigment in the detection of polarized light. *Vision Res*. 1980;20:213–220.
56. Stanworth A, Naylor EJ. Haidinger's brushes and the retinal receptors; with a note on the Stiles-Crawford effect. *Br J Ophthalmol*. 1950;34:282–291.
57. Summers DM, Friedmann GB, Clements RM. Physical model for Haidinger's brush. *J Opt Soc Am*. 1970;60:271–272.
58. Fairbairn MB. Physical models of Haidinger's brush. *J R Astron Soc Can*. 2001;95:248–251.
59. Hallden U. An explanation of Haidinger's brushes. *AMA Arch Ophthalmol*. 1957;57:393–399.
60. Charbel Issa P, Heeren TF, Kupitz EH, Holz FG, Berendschot TT. Very early disease manifestations of macular telangiectasia type 2. *Retina*. 2016;36:524–534.

Investigative Ophthalmology & Visual Science